cosine | research

cosine

High-Performance X-ray Optics

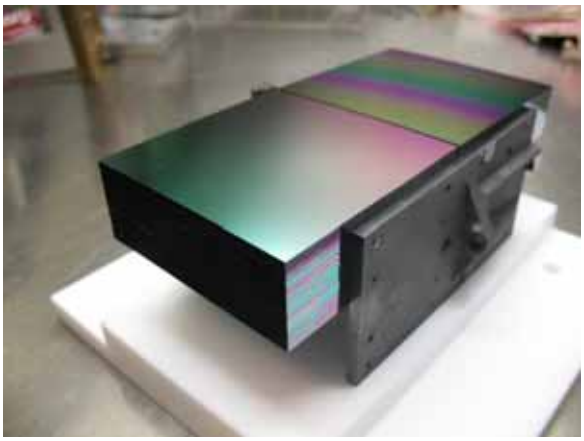

Abstract and Summary report

Document id	cR-SPO-SummaryReport
Issue	1
Date	2010-04-02
Pages	31
Copyright	© 2010 cosine Research BV

Approved	M. Collon cosine Research BV	

Changelog

Date	Issue	Author(s)	Description
2010-04-02	1	M. Collon	First issue

cosine research bv | Niels Bohrweg 11 | 2333 CA Leiden | The Netherlands
Tel. +31 71 5284962 | Fax +31 71 5284963 | E-mail info@cosine.nl | Internet cosine.nl
Chamber of Commerce Rijnland 28091022 VAT NL809835149B01
ING Bank 67.33.21.932 IBAN NL70INGB0673321932 BIC INGBNL2A

Table of Contents

1 Abstract

An ESA TRP activity was carried out by cosine Research (NL), Micronit (NL), Kayser-Threde (DE), SRON (NL), DTU (DK) and MPE (DE) with the goal of improving the angular resolution of Silicon Pore X-ray Optics. Silicon Pore Optics is the European baseline mirror technology for the International X-ray Observatory (IXO), one of the three L-class mission candidates under the Cosmic Vision 2015-2025 program.

The entire production chain of these light-weight and modular X-ray optics has been reviewed, improved, demonstrated and tested, from silicon plate manufacture, over ribbing, dicing, wedging, coating, stacking, assembly and integration up to petal level.

A simplified process flow to manufacture stackable Si mirror plates is demonstrated, with an emphasis on reduced manufacturing cost. An important factor is the consideration of standard wafer processes and equipment. This activity has shown ways to enable manufacturing the required 200 000 silicon plates for IXO in a cost-effective manner within the allocated time-scale.

Customized wedging equipment is used to taper plates to the correct geometry, and industry-standard oxidation and wet chemical processes are used to ensure bondable surfaces. An analysis of the relevant tolerances has led to the optimization of the wedging process in order to meet the requirements of the IXO.

Two methods to apply structured coatings have been developed and stacks with Ir and C overcoating were demonstrated. Reflectometry measurements were performed to demonstrate that the silicon plates, after all processing steps and including coating have a rms surface roughness of 0.5 nm.

A new generation of the automated stacking robot has been developed. Using this robot, stacks with a radius of curvature of 2 m consisting of fully wedged plates have been built and were measured at the BESSY synchrotron radiation facility.

The complete first plate exhibits in single reflection a HEW of 4.2”. In double reflection a HEW of 9” on the first 4 plates and 16” on the first 20 plates was measured on mirror modules mounted in flight representative configuration. This compares to 17” on the first 4 unwedged plates measured in 2007 and demonstrates the significant improvement in stacking quality.

The activity was centred on improving the technology at a radius of 2 m for a focal length of 50 m, conform the initial requirements. At the end of the project, a detailed study on the requirements to produce modules at inner radii and shorter focal length has been carried out. First considerations about inner radii modules as required for IXO and re-calculation of effects of launch loads on mirror modules were all concluded successfully.

So far no show stopper has been identified that would impede improving the performance of silicon pore optics beyond 5”.

1.1 Abbreviation list

AD	Applicable Document
BESSY	Helmholtz-Zentrum Berlin für Materialien und Energie - Speicherring BESSY II
Con-X	Constellation-X
DTU	Danish Technical University
FCM	Four-Crystal Monochromator beamline of PTB at BESSY
FEM	Fixed Energy Monochromator beamline of PTB at BESSY
HEW	Half Energy Width
HPO	High-performance pore optics
IXO	International X-ray Observatory
KT	Kayser-Threde
MEMS	Micro Electro-Mechanical Systems
MPE	Max-Planck-Institut für extraterrestrische Physik
PDS	Particle Detection System
PTB	Physikalisch-Technische Bundesanstalt
PSF	Point Spread Function
RD	Reference Document
R&D	Research and Development
SME	Small-medium size enterprise
SPO	Silicon Pore Optics
SRON	Netherlands Institute for Space Research
TRL	Technology Readiness Level
TTV	Total thickness variation
XEUS	X-ray Evolving Universe Spectroscopy
XOU	X-ray Optical Unit

2 Introduction

Silicon pore optics is a technology developed to enable future large area X-ray telescopes, such as the International X-ray Observatory (IXO), a candidate mission in the ESA Space Science Programme 'Cosmic Visions 2015-2025'. IXO uses nested mirrors in Wolter-I configuration to focus grazing incidence X-ray photons on a detector plane. The IXO mirrors will have to meet stringent performance requirements including an effective area of ~3 m^2 at 1.25 keV and ~1 m^2 at 6 keV and an angular resolution better than 5 arc seconds. To achieve the collecting area requires a total polished mirror surface area of ~1300 m^2 with a surface roughness better than 0.5 nm rms. By using commercial high-quality 12" silicon wafers which are diced, structured, wedged, coated, bent and stacked those performance requirements of IXO can be attained without any costly polishing steps. Two of these stacks are then assembled into a co-aligned mirror module, which is a complete X-ray imaging system. Included in the mirror module are the iso-static mounting points, providing a reliable interface to the telescope. Hundreds of such mirror modules are finally integrated into petals, and mounted onto the spacecraft to form an X-ray optic of four meters in diameter.

This ESA TRP funded activity 'High Performance X-Ray Optics' was an activity that started late 2007, directly following a project which had resulted in the very first X-ray mirror module ever made from Silicon Pore Optics, with a measured X-ray performance of 17" half-energy width (HEW) on the first 4 plates.

The activity is based on developing mirror modules with an improved angular resolution, still with a focal length of 50 m and an outer radius of 2 m. We concentrated the development effort on the basic element, the stack, being the most critical element. A number of targets were set to mature the technology readiness level (TRL):

1. Point Spread Function (PSF) improvement
2. First steps towards industrialisation of the mass production process
3. Development of high energy coatings

Significant effort was spent on further improving on the figure of the optics, which is mainly determined during stacking.

Four major topics were tackled in this activity:

1. The silicon plate manufacture was taken over by Micronit, resulting in a new generation of ribbed plates. The technological step of applying wedges was also mastered and a number of different methods were demonstrated on application of wedges.
2. It was successfully demonstrated that structured Ir+C coatings can be applied to wedged plates, which were subsequently stacked and characterised under X-rays. Two methods were developed, one employing metallic masks and one using lithographic techniques.
3. The finite element models were further detailed, resulting in a deeper understanding of number of effects to be considered when progressing to stack inner radii modules in the near future.
4. A completely new stacking robot was set up, replacing the previously used linear concepts with a central robotic arm, able to be expanded in the future with new modules. Advanced plate cleaning and activation systems were installed and tested and a flexible former was developed, allowing studying the dynamics of the stacking process in situ. The stacking process was completely automated, resulting in a consistent quality of the produced stacks.

This activity has resulted in a second generation of mirror modules, having on the first 4 plates a measured X-ray performance of 9" (HEW) and 16" HEW on the first 20 plates, laying the ground to reach the desired 5" angular resolution in the near future.

The activity also fell into a period where ESA performed a first system study and XEUS was merged with Con-X, resulting in IXO. This meant that the focal length requirement reduced from

50 m over 35 m to 20 m and that the outer and inner radii were reduced to 2 and 0.3 m, respectively. Besides maintaining the main objectives of this activity, this resulted in additional resources to be spent on the development of larger wedge angles, on first considerations about inner radii modules and re-calculation of effects of launch loads on mirror modules, which were all concluded successfully.

The consortium executing the work consisted of:

cosine, a Dutch small-medium size enterprise (SME) that has a long history of technology development for ESA, priming this activity. cosine's personnel have extensive experience both in the development of software for scientific applications and the design, construction, and testing of scientific instruments for space applications. cosine has lead since 2002 the development of Silicon Pore Optics. The stacking of ribbed silicon plates is based on a metrology and assembly tool that has been developed and built by cosine.

Micronit, a Dutch SME specialised in etching and patterning glass and silicon structures, who took over silicon plate production from a german supplier. Micronit has significantly simplified the production process and had the task of developing a suitable wedging process for the plates.

The **Danish National Space Centre**, part of the Danish Technical University, is heading a development program of depth graded multilayer coatings to extend the energy band of future X-Ray telescopes up to and beyond 100 keV. This led to the involvement in the early definition stages of ESA's XEUS mission study and subsequent contract work to study a possible high energy extension of the IXO mission using this technique. The DNSC was responsible for the development of a masked coating process for ribbed silicon plates.

Kayser-Threde has a broad experience in developing space-borne scientific payloads and has designed, manufactured and successfully qualified eight units of the XMM-NEWTON x-ray mirror modules. For the development of Silicon Pore Optics KT has designed and manufactured a CeSiC® petal for the integration of XOUs into a larger telescope structure. KT also manufactured the CeSiC® petal elemental cell and provided technical support.

SRON, with its expertise in X-ray astronomy and development of X-ray instrumentation, supported the study team in achieving a thorough understanding of the mechanics of the stacking process.

MPE, has special expertise in the design, development, and calibration of X-ray astronomical optics and has supported the study team by providing their X-ray test facility PANTER and resources to analyse the data.

3 Silicon Pore Optics

Silicon Pore Optics use commercial, double-sided polished high-grade 12" wafers which are mass-manufactured by the semi-conductor industry and which have the required surface roughness and flatness to form X-ray optics. Using established mass production processes the individual mirrors are first diced from a wafer and then the backside is grooved, which leaves a thin membrane and a number of ribs (Figure 1). Parameters like the membrane thickness, the rib pitch, the rib width, the plate width and its length can all be adjusted to optimize the optical performance or the mechanical behaviour of a stack. To reduce stray-light the sidewalls are made non-reflective during production.

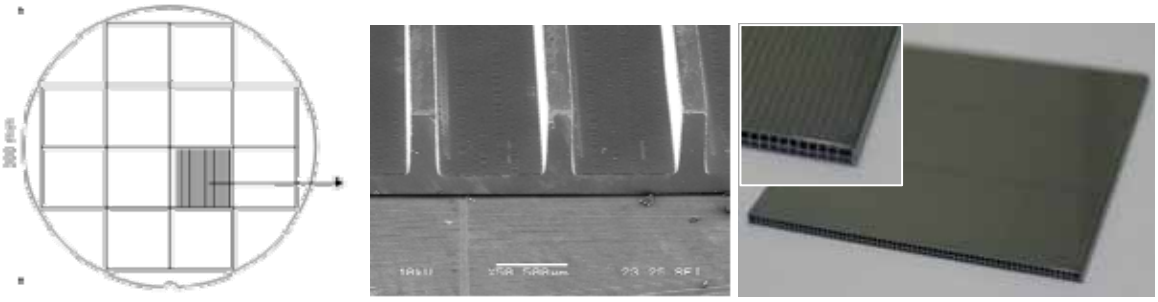

Figure 1 (left) Silicon Pore Optics are made from commercial high-quality 12" silicon wafers which are diced into plates. (middle) The plates are ribbed (reflecting surface pointing downwards). The 0.17 mm wide ribs have a pitch of 1 mm and the membrane is 0.17 mm thick. The plates are then wedged along the rib direction (not shown) and a patterned iridium coating is applied on the reflective surface (right). The pattern keeps the areas free where the next plate will be bonded. The plate shown has dimensions of 66 x 66 mm^2 and a thickness of 0.775 mm.

The mirror plates are then cleaned and elastically bent into a conical shape, using a fully automated stacking robot. The mirrors remain flat along the pores since the Wolter-I geometry of a parabolic and a hyperbolic mirror can, for long focal lengths, be approximated by two cones ('conical approximation'). The achievable angular resolution is then limited by the height of a single pore. In the case of IXO with a focal length of 20 m and using pores with a height of 0.6 mm this results in a lower limit to the HEW of about 3". To reduce the lower limit we explore shaping the mirrors also in longitudinal direction. Using the same automated assembly robot the plates are then aligned and stacked by direct silicon bonding (Figure 2) onto a silicon mandrel. Note that only the figure of that mandrel is replicated, not its roughness. Multiple mirrors form together a stack, in which the X-rays are reflected off the reflective membrane inside a pore. Due to the inherent stiffness of the stacks, the figure of the individual mirrors remains preserved during further mounting and integration. Two of such stacks are co-aligned and integrated into brackets to form a so-called mirror-module.

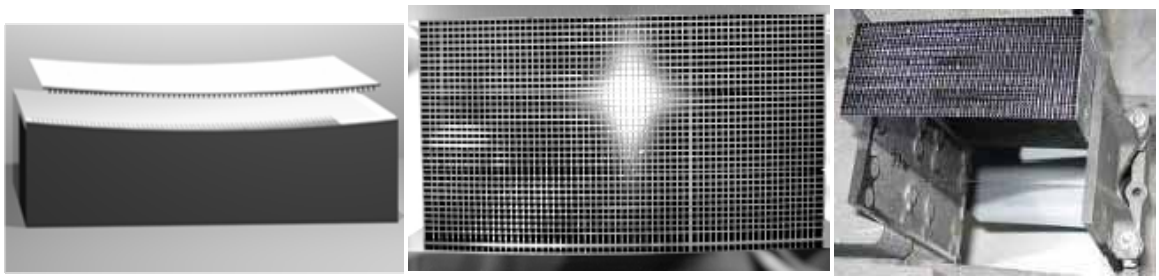

Figure 2 The ribbed, wedged and coated silicon plates are elastically bent into cylindrical or conical shape (left). 45-70 of such plates are stacked on top of each other (middle) by an assembly robot. Two of such stacks are co-aligned and integrated into a mirror module and mounted inside a petal (right).

4 Plate production

4.1 Introduction

The plate manufacturing process begins with semiconductor industry standard 300mm wafers, and ends with diced, ribbed, wedged, and coated plates which can be subsequently stacked to form an optical unit. Silicon pore optics are currently fabricated using a combination of established MEMS fabrication techniques and novel fabrication techniques specifically designed for IXO. The scientific community has specified requirements of an angular resolution of 5 arc-seconds and an effective area of 3 square meters, and the R&D effort to date has focused on achieving these goals and eliminating the most significant sources of error.

The production of silicon mirror plates consists of dicing 300mm wafers into rectangular plates, ribbing the plates to create grooves along the optical axis, wedging the plates to create a thickness taper along the optical axis, and coating to provide a patterned metal coating on the reflective surfaces. In Figure 3 a schematic illustration of the process flow used to dice the 300mm wafers into 12 square plates is shown, and the subsequent ribbing, wedging, and coating steps are also illustrated.

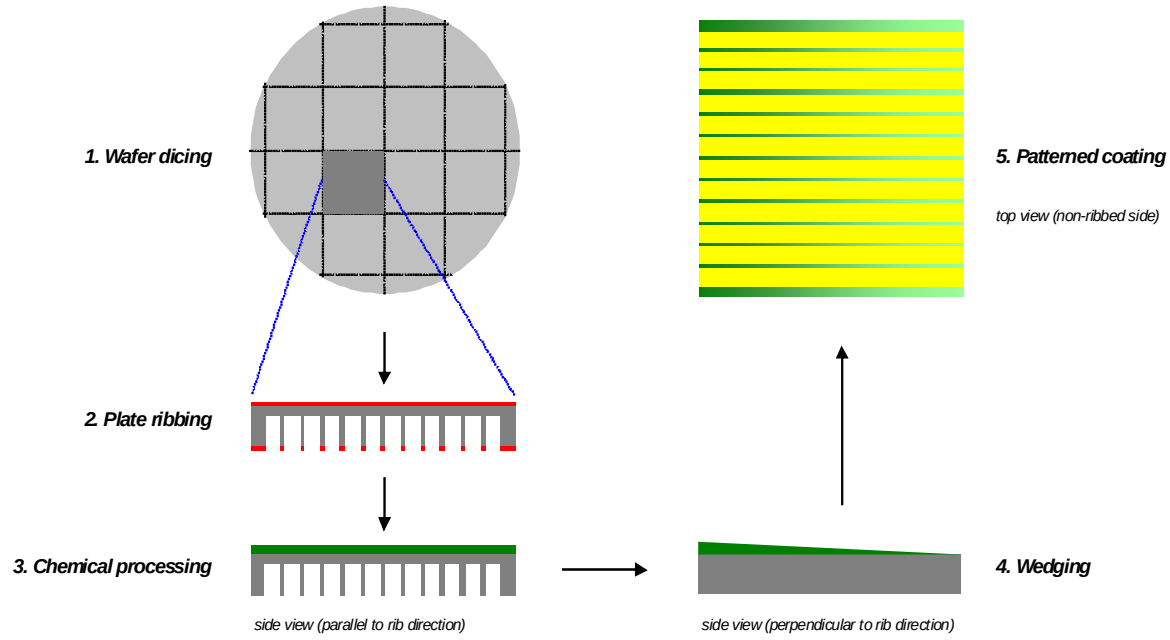

Figure 3 Schematic overview of process flow for production of Si mirror plates.

4.2 Silicon mirror plate requirements

The quality of a silicon pore optics plate can be categorized by its X-ray reflectivity, mechanical geometry, and bondability. The X-ray reflectivity is determined solely by the surface roughness and material properties of the reflective surface. The mechanical geometry of an individual plate will determine the optical properties, stiffness of an HPO, ruggedness, effective area, mass, and will also have some effect on bondability. The bondability can be characterized by bonding strength, which is a combination of many surface properties and particle contamination.

The X-ray reflectivity was measured for various material surfaces including double-side polished silicon and fully processed thermal oxide. In Figure 4 the processed thermal oxide layer is

demonstrated to be equally reflective as the silicon starting material. Bondability of these thermal oxide layers after the wedging process further demonstrates their suitability for use in silicon pore optics.

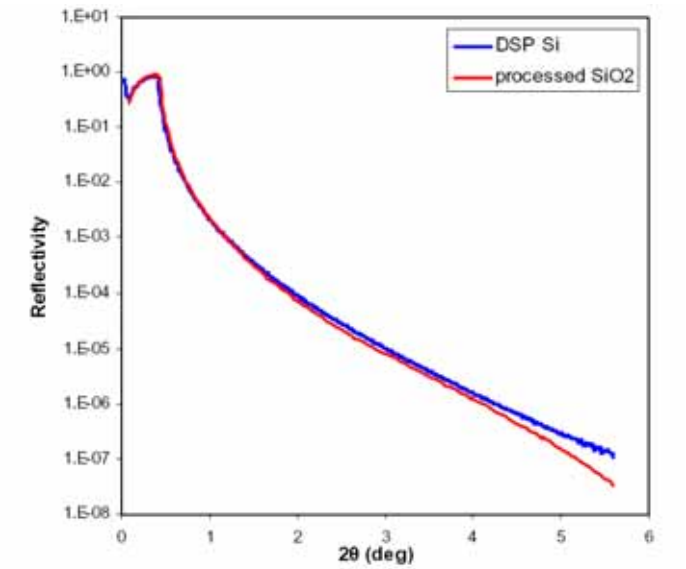

Figure 4 Measured X-ray reflectivity at an energy of 8 kev of commercial off-the-shelf double-side polished (DSP) 300 mm Si wafers and processed SiO_2 plates.

The initial starting wafers are SEMI-standard surface, 775 micrometer thick, 300 mm diameter wafers which are double-side polished. These wafers are subsequently ribbed, oxidized and wedged. The plates are cut from a <100> p-doped Si crystal, and ribs are cut along the <100> crystal direction.

The current SPO optical design for the IXO is a conical approximation to a Wolter-I optic. In this design, incoming X-rays make 2 reflections, one off a conical approximation to a parabolic surface and one off a conical approximation to a hyperbolic surface. The Wolter-I design is well-suited to a monolithic mirror design such as the IXO due to the fact that the tolerances on the relative position and angle between the two reflecting mirrors is very strict, but the telescope resolution is less sensitive to deviations in radius, position, and angle of the mirror pair with respect to the detector. The silicon plate parameters such as plate thickness, plan-parallelism, and wedge angle influence the resulting resolution of the optics. We therefore focus our efforts on improving the precision of these parameters, in particular the wedge angle.

For silicon pore optics the plate bondability is essential for obtaining a rugged and durable mirror stack. Silicon wafer surfaces can be bonded either by hydrophilic or by hydrophobic bonding. Hydrophobic bonding occurs between two silicon layers which are typically made by removing the native oxide. Hydrophilic bonding occurs between two oxide layers, which can be native oxide layers of a few angstroms in thickness, or thermal oxide layers of hundreds of nanometers. The bond energy of room temperature direct bonded wafers is highest for hydrophilic silicon i.e. native oxide (83 mJ/cm^2), thermal oxide (52 mJ/cm^2), and lowest for hydrophobic Si (10-20 mJ/cm^2). This bond energy is increased up to 2000 mJ/m^2 if the bonded stacks are annealed. We currently bond thermal oxide to thermal oxide surfaces.

4.3 Silicon mirror plate process flow

4.3.1 Wafer dicing and plate ribbing

After wafer dicing the plates are coated with a protective layer in order to avoid damage to the Si surface during ribbing and wet chemical processing. During the ribbing process of the mirror plates, grooves are diced in the Si substrate to create the pores for X-ray optics. The grooves form the empty space for X-rays to pass through, whereas the ribs provide the required structural stiffness to the optical units. Since the mirror plates will be curved in the stacking process to the radius of the telescope, the remaining plate membranes need to be as thin as possible. The plate membrane thickness thereby determines the flexibility of the plates. The ribs support the individual mirrors at the appropriate distance and curvature. The top side of the ribs will be bonded to the mirror surface of another silicon mirror plate. Plates are stacked to the necessary amount to form a self-supporting monolithic structure. A schematic picture of the mirror plate ribbing geometry is shown in Figure 5.

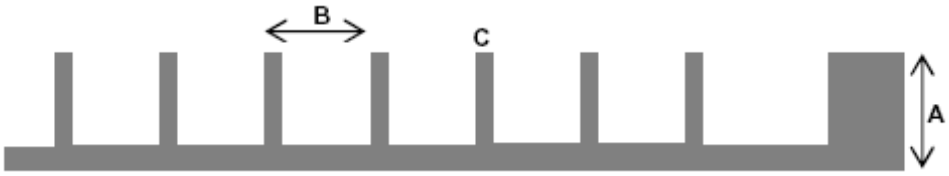

Figure 5 Schematic picture of the plate rib geometry; plate thickness (A) = 0.775 mm, pitch (B) = 1.0 mm, rib width (C) = 0.17 mm.

Although the plate ribbing process results in a well-defined pore geometry, a known side effect of dicing is the generation of micro-cracks in the material. Therefore, a second step in the shaping of the required rib geometry is applied in order to remove any residual micro-cracks, referred to as a damage etch.

A potassium hydroxide (KOH) solution is used to anisotropically and selectively etch damaged silicon material inside the diced grooves, while a protective coating is preventing the top surface of the ribs from being etched (see also Figure 3). Although the surface of the diced grooves remains rough after damage etching, this will not affect the optical performance of the telescope. In contrast, surface roughness within the grooves helps to scatter unwanted X-rays. Figure 6 and Figure 7 show side views of the plate rib geometry obtained after damage etching. Since one has full access to the pores during manufacturing of the plates, one could also apply other surface roughening techniques to further reduce stray-light.

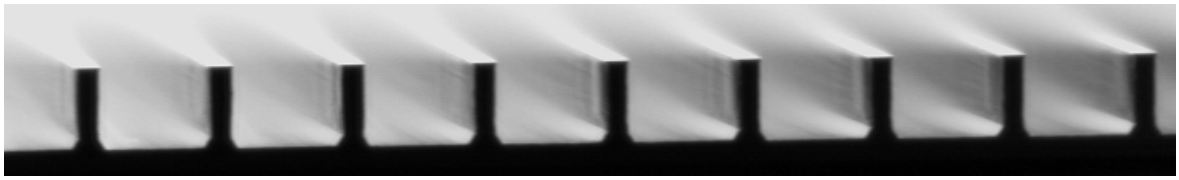

Figure 6 Side view of a ribbed and damage etched Si plate.

The plates are then thermally oxidized to create a uniform SiO_2 layer in preparation for the wedging process.

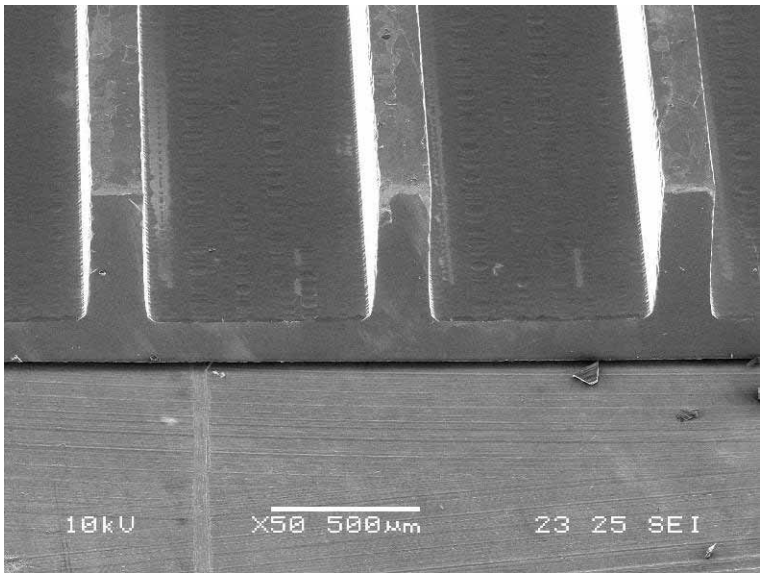

Figure 7 SEM photograph (side view) showing the edge of a ribbed and damage etched Si plate.

4.3.2 Wedging

The goal of the wedging process is to taper plates along the optical axis so as to create a conical approximation to a Wolter-I Optic.

The achievable manufacturing tolerances of silicon mirror plates influence the maximum achievable performance of the IXO telescope. We show that both plan-parallelism and wedge angle must be carefully controlled to ensure that the 5 arc-second resolution requirement is met. The preliminary calculations that we describe below are all based on simple trigonometric principles, and more detailed 3D computer simulations are being developed to consider more potential sources of error simultaneously. For the purposes of calculations, the focal length is assumed to be 20 m.

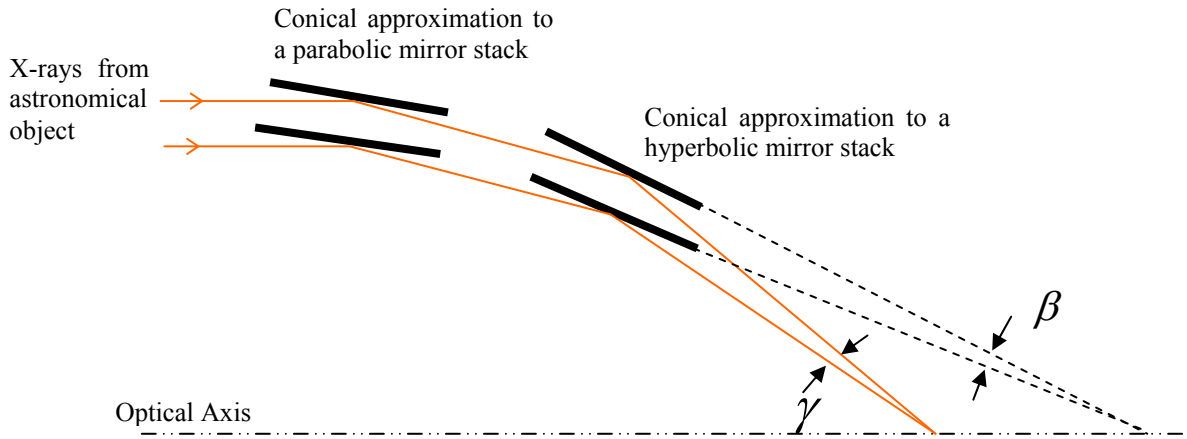

Figure 8 Schematic diagram of X-ray reflections on two stacked plates (not to scale).

We define the wedge angle between two adjacent plates in the parabolic stack as α, the wedge angle between adjacent plates in the hyperbolic stack as β and the resulting difference in reflection angles between two adjacent rays is equal to γ. In Figure 8 a schematic illustration of two stacks of 2 silicon mirror plates is shown in conical approximation to the parabolic/hyperbolic part of a Wolter-I optic (α is not shown).

If there is a manufacturing error in the angle β between two consecutive plates in an IXO mirror module, the beams from two consecutive pores will overlap slightly before or slightly beyond the desired focal point. An error in the wedge angle β will therefore slightly deteriorate the angular resolution of the telescope. The sensitivity of the angular resolution to such an error in wedge angle is equal to:

$$\frac{\partial\gamma}{\partial\beta} = -\frac{\partial\gamma}{\partial\alpha} = 2 \tag{1}$$

We have measured the standard deviation of manufactured wedge angles which have been produced to date to be less than 3% by means of ellipsometry and note that we are currently improving the process to reduce this error to under 0.5%. In this example calculation we take the wedge angle error of a hyperbolic wedge of 6 arc-seconds to be 3%, and calculate the corresponding angular resolution of a stack of two plates to be:

$$\Delta\gamma \approx 2\times\Delta\alpha = 2\times(0.03\times 6.0 arc-\sec) = 0.36 \text{ arc-seconds} \tag{2}$$

For parabolic plates, the error in resolution due to deviations in wedge angle is:

$$\Delta\gamma \approx 2\times\Delta\beta = 2\times(0.03\times 2.0 arc-\sec) = 0.12 \text{ arc-seconds} \tag{3}$$

With the calculations above, it is shown that accurate control of the mirror plate wedging angles is required to maintain the angular resolution. The compounding effect of the stacking process on all sources of error is currently under investigation by means of more advanced optical ray-tracing, but we note that the errors are normally distributed about the mean value and are therefore not linearly cumulative in a stack.

In the case of a 0.5% error in the wedge angle, which has already been demonstrated in the most recent batches of mirror plates, these errors are reduced to 0.06 arc-seconds for the hyperbolic stack and a mere 0.02 arc-seconds for the parabolic stack. We note that the wedging angle errors are normally distributed about the mean value for the wedge angle and are therefore not linearly cumulative in a stack. The compounding effect of the stacking process on all sources of error is currently under investigation by means of more advanced X-ray-tracing, but our preliminary calculations show that the achievable wedge angles are within the range and accuracy required to produce optics with the resolution required for the IXO.

Compensation for the Natural Wedge

The calculations above do not take into account the initial plan-parallelism error, or 'natural wedge,' of the silicon mirror plates. The error induced by this natural wedge could be reduced by utilizing existing manufacturing techniques such as magneto-rheological polishing to reduce the total thickness variation to under 40 nanometers over a 300mm wafer. However, to reduce manufacturing cost, we are currently investigating a measurement of the natural wedge using existing interferometric methods and a subsequent adjustment of the wedge angle in order to compensate for the natural wedge.

Wedging process

An ellipsometer with an automated stage is used to measure the thickness of the wedge layer across the entire length of a plate before and after wedging (see Figure 9). By measuring the thickness of the oxide layer before wedging, any errors in the angle of the original oxide layer can be linearly compensated for by adjusting the wedging process parameters. This same technique that we have developed for compensation of a natural wedge in the oxide layer could be applied in the future to compensate for natural wedges present in the Si wafer if a TTV measurement technique is introduced into the process.

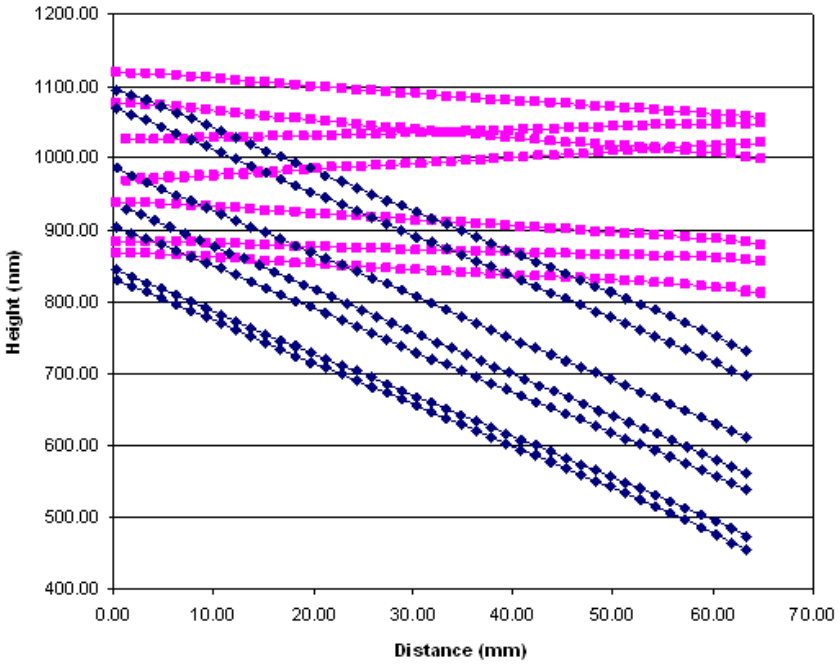

Figure 9 Oxide height as a function of distance along optical axis before (pink) and after (blue) wedging for 7 different Si plates.

Figure 10 shows a schematic 3D picture of ribbed, wedged and stacked Si plates as well as a photograph of the wedged reflective side and non-wedged ribbed side. The color pattern clearly indicates the thickness gradient of the oxide layer along the optical axis of the plate. If larger thickness tapers are desired in the future, for plates in the inner radius, a similar wedging process as described above can be applied to create a double-side wedge on the mirror plate. A typical example of a double-side wedged plate is shown in Figure 11.

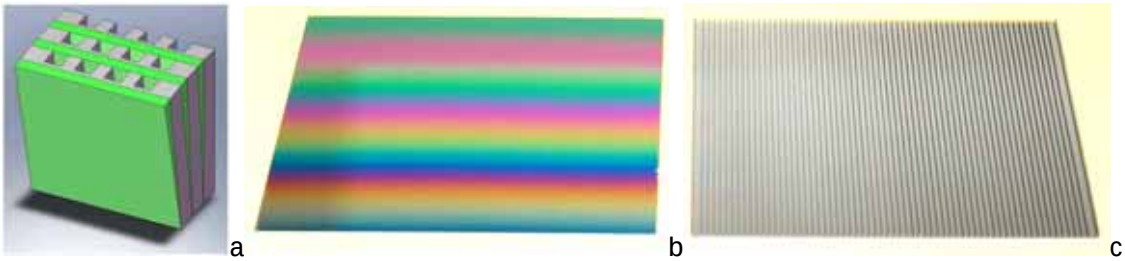

Figure 10 Single-side wedged plates: schematic 3D picture of stacked Si plates (a), photographs of wedged reflective side (b) and non-wedged ribbed side (c).

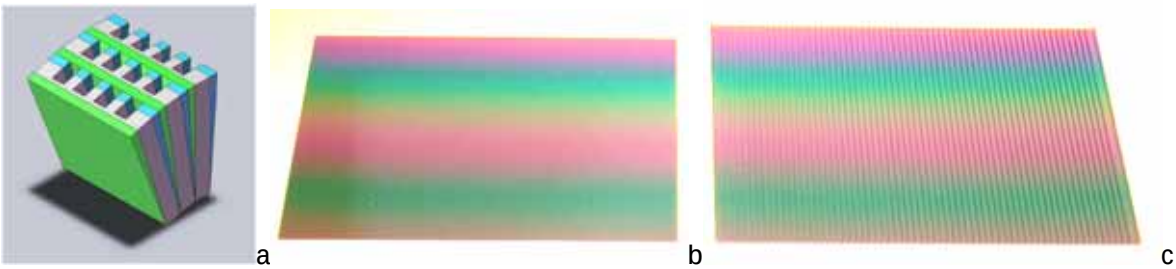

Figure 11 Double-side wedged plates: schematic 3D picture of stacked Si plates (a), photographs of wedged reflective side (b) and wedged ribbed side (c).

4.4 Industrialization

In the previous sections we have described a simplified process flow to produce silicon mirror plates. The entire process is based on standardized semiconductor and MEMS technology and is currently performed in a facility used for mass-production of silicon and silica devices. The process, which requires only a limited amount of cleanroom space (approx. 500 m^2), has been designed such that it can be scaled up to high-volume batch processing.

The current processing time for production of 45 mirror plates (one stack) is in the order of 6-8 days, limited by the large amount of single plate handling (e.g. dicing, lithographic processing) and the time consuming plate ribbing process (10-15 min per plate). The ESA technology development for SPO includes partial industrializing of this process flow (e.g. batch processing, process automation) by 2011. Using commercially available semiconductor equipment such as a series of dicing saws running in parallel with dual-spindle dicers, automated wet-benches and automated quality control, the total production can be substantially increased to hundreds of plates per day.

5 Coating development

5.1 Introduction

In order to achieve a good reflectivity and hence effective area in the range of 1 keV up to 10 keV, the Si plates that make the optics of IXO have to be coated with a layer of high Z material and then a layer of low Z material to smoothen out the effects of absorption edges in the high Z material and increase the effective area below 3 keV. It is however crucial that after this coating, the plates are still able to form Si-Si bonds in order to build stacks. This requires that there is no coating on the ribs of the silicon plates or on the area on the top of the silicon plate where the ribs are going to bond

Three approaches of coating the silicon plates have been evaluated in this project: Masked coating, where one physically masks the Si plates during the coating process in order to keep specific areas of the Si plates free of coating. Lithographic coating, where a photoresist protects the not-to-be coated areas during the coating process. The third approach was to deposit a thin layer of Si on the (unmasked) coating to render the plates bondable again.

5.2 Coating materials and x-ray testing

The silicon plates were coated at DTU-Space. The coating is done in a DC magnetron sputter facility. For high Z material we used Ir with a density of 22.5 g/cm^3. For low Z material we used C.

To evaluate the thickness of the C top layer we have compared three samples with different C overcoat thicknesses, all measured in the energy range from 1.7 keV and to 10 keV at the FCM beamline at BESSY. From Figure 12 it is clear that the reflectivity in the range from 2 keV to 4 keV improves strongly by the addition of a C top layer. From this figure it is also clear that different C thicknesses give a small decrease in reflectivity compared to the Ir coating without a C top coating in the energy range between 4 keV and 8 keV depending on the thickness of the C layer. What is considered the optimal coating thickness for Ir and C will depend on the specific requirements coming from the scientific community. We therefore do not classify any of the coating thicknesses as optimal. The coatings of different thicknesses are only used to demonstrate the capabilities of the coating process, and to evaluate the roughness of the different coating thicknesses and materials.

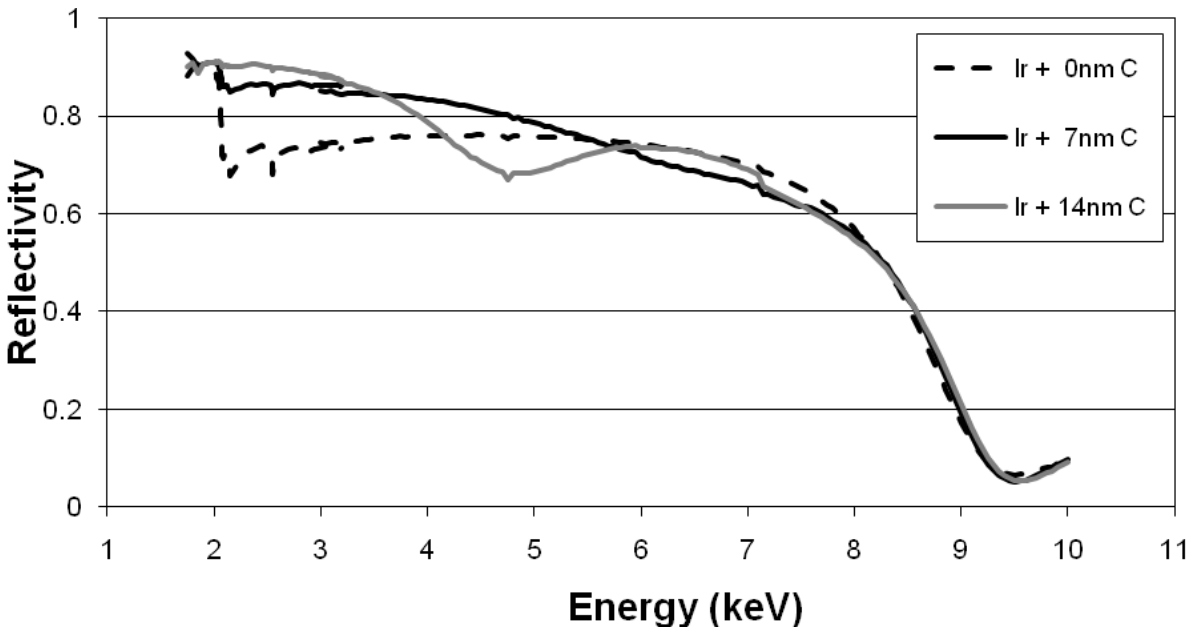

Figure 12 X-ray measurements of the coated Si plates with different thickness of the C top layer. The measurements are made at 0.575 degree and the Ir thickness is about 14 nm. The drop in reflectivity at 7 keV could indicate some contamination with Fe in the coating.

5.3 Masked coating

The mask is laser cut out of a 1.25 mm thick stainless steel plate and is 70.0 mm x 70.5 mm wide with metal ribs of 0.3 mm width and a 1 mm pitch, identical to the rib pitch of the Si plates. These metal ribs mask the areas on the Si surface where later the ribs of the backside form the next Si plate will bond. To keep the metal ribs straight there are in the transversal direction two 0.2 mm wide support ribs placed perpendicular to the long metal ribs, with a 22 mm spacing. The total area which is not coated due to these transversal ribs is 19 mm^2 (about 0.6% of the total area of the Si pore optic). A picture of the mask is shown in the left center of Figure 13.

Since the mask and the mounting jig are made of stainless steel, there can be no contact between these and any area on the Si plate to prevent damaging the reflective surface. Figure 11 shows a setup that holds the metal mask at a small distance to the silicon plate. To align the mask to the ribs infrared light was used, to which silicon is transparent (see Figure 14).

The ribbed Si plates have been coated with a Ir + C coating using the masking setup in the DC magnetron sputter facility at DTU-space. After coating, the Si plates were removed from the coating jig, repacked and returned to cosine for inspection and bonding trials. Figure 15 shows a coated masked Si plate. The darker areas are the masked (non-coated) areas. The masked areas used for bonding are running vertically in this image. The two horizontal lines are the masked areas due to the support ribs that run across the mask.

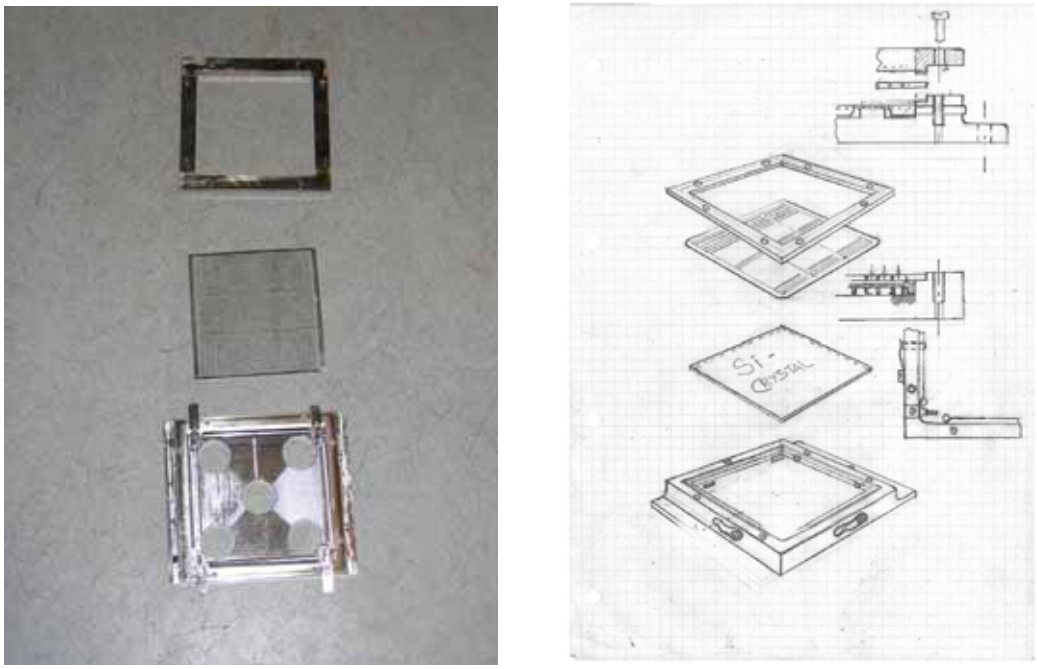

Figure 13 Picture (left) and schematic drawing (right) of the mounting jig that holds the Si plate and the mask.

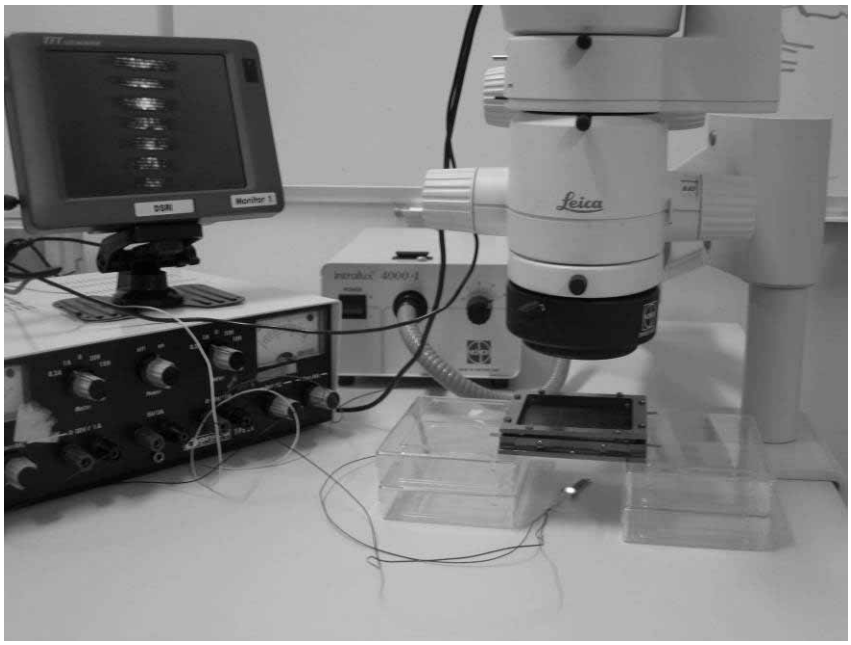

Figure 14 Picture of the alignment setup.

Two bonding trials have been performed. The first test has been performed to validate the shipping and handling of the plates during the coating process, but excluding the masking and coating itself. In the second trial plates were shipped to DTU-Space for masked coating. All plates were coated there with Ir and C, leaving bare Si areas under the mask. The plates were subsequently bonded together with good result and then immediately taken apart again for the X-ray measurements with synchrotron radiation at the PTB four-crystal monochromator (FCM) beamline at BESSY II. After the measurement campaign at the BESSY facility, the same two plates were activated again, and bonded in the same geometry as described above, see Figure 15. These coated masked mirror plates are now permanently bonded.

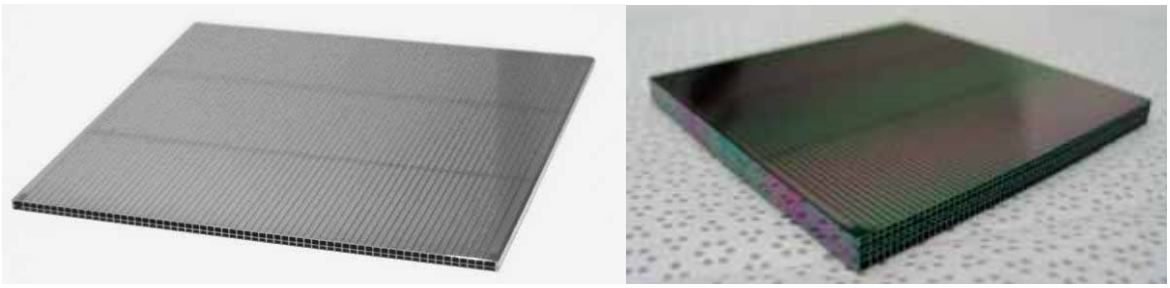

Figure 15 The first coated unwedged (left) and wedged (right) stacked Si pore optics. The contrast in the left picture has been manipulated to make it easier to distinguish the coated and the uncoated area (the dark lines).

In Figure 16 we show an energy scan of the "uncoated area" and the coated area at an angle of 0.575 degree. We also show the calculated energy scan for a 6 nm Ir coating and a 11 nm C top coating and a bare Si surface. The roughness of the Ir coating in the calculation is 0.4 nm and the roughness of the C layer is 0.7 nm. The reflectivity of the coated area is lower than the calculated values in the whole energy area from 2 keV and up to 6 keV. This can not be explained with either the thickness or the roughness of the Ir or C layer. A decrease of the Ir thickness will drop the reflectivity in the 6 to 8 keV area below the measured values but only has a modest effect at lower energies. By changing the thickness of the C layer, the local minimum around 5 keV will move to towards lower or higher energies (see Figure 12). An increase of the C roughness is nearly not visible on the reflectivity curve and an increase of the roughness of the Ir will lower the reflectivity mostly at energies above 5 keV. We note that a roughness of 0.4 nm for the Ir coating is a rather conservative estimate since we have also Ir coated silicon plates that were exhibiting a lower roughness. Because the measurement of the "uncoated area" included some of the coated area (the slits clipping the illumination area were not small enough) the measured data is higher than for the calculated bare Si.

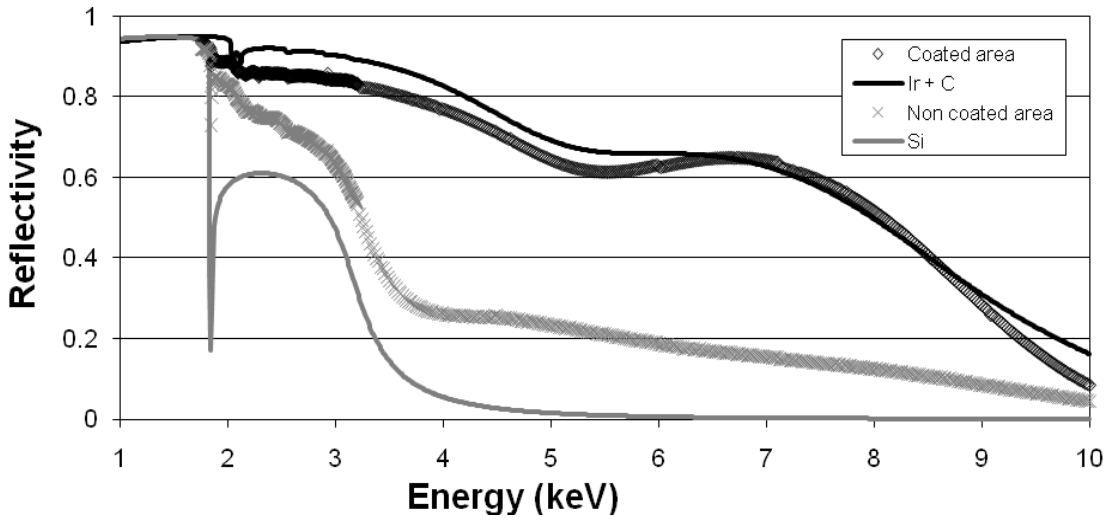

Figure 16: X-ray measurements of the coated and the not coated area of a Si plate. The measurements are made at 0.575 degree.

5.4 Si overcoat

Since the masking of the Si plates is complicated and labour intensive, an alternative method to produce a bondable coated plate was proposed. This alternative method consisted of adding a thin layer of Si on top of the Ir and C coating, in order to bond the ribs of the next Si plate to

that new Si layer. But even a 1 nm Si coating on top of the Ir + C coating reduces the reflectivity of the underlying coating in the whole energy range and is therefore not a viable option.

5.5 Patterned reflective coating

An alternative process for patterning the reflective side of the mirror plates is the use of standard photolithographic techniques as applied in the semiconductor industry. Patterning of the reflective side with a photoresist coating eliminates the use of a sputtering mask during the metal coating process. After sputtering, the excess metal which is coated in the bonding areas can be easily removed by a lift-off process. The edge definition of the resulting patterned coating is very accurate as shown in Figure 17. Further research to optimize the photoresist coating process and to improve the bondability of patterned mirror plates is ongoing.

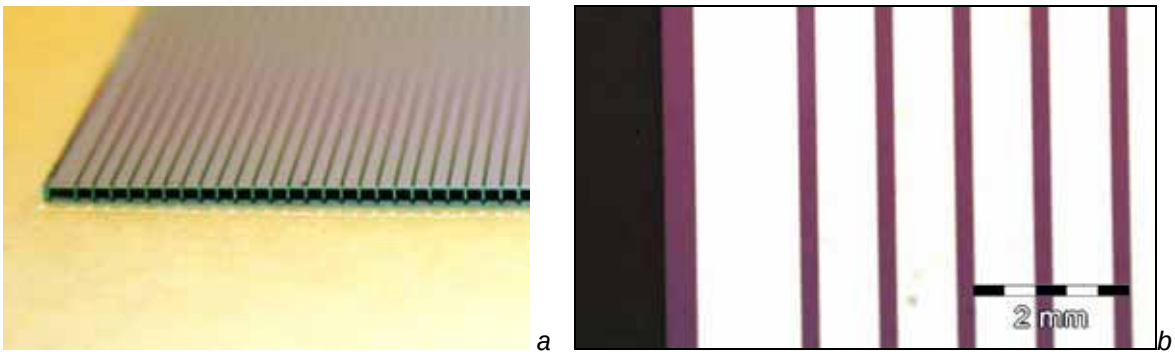

a b

Figure 17 Lithographically patterned metal coating on the reflective side of the Si mirror plate: photograph of the plate edge (a), microscopic photograph showing (bright) metal coated reflective areas and (dark) non-coated bonding areas (b).

6 Stack production

At the beginning of this project the stacking robots were able to achieve on 4 plates a HEW of 17". The understanding was that this limitation was mainly caused by incomplete bonding of the plates, caused by

(a) particulate contamination during stacking and

(b) a shape mismatch of mating plates at their outer edges.

In this project the entire production chain from plate manufacture, over cleaning and stacking to XOU integration was reviewed with the aim to reduce particulate contamination and to improve the bonding of stacks. To achieve this, cleaning and stacking processes needed to be adjusted. In this chapter we report which changes to the process have been implemented and which stacking results we obtained with the newly developed process.

6.1 Stacking process

The shape match between plate *n* and *n+1* is considered, besides cleanliness, one of the most important figures of merit in the stacking process. An error in shape match during bonding can limit the bonded area, which has negative impact on the next stacked plates as the debonded area grows inwards, as shown in Figure 18.

The shape of two mating plates is basically defined by the mandrel and by the die. The figure of the mandrel is accurate to 0.1" and thus sufficiently good. Therefore the effort concentrated on improving the figure of the die by introducing force sensors to measure in situ the force distribution during stacking.

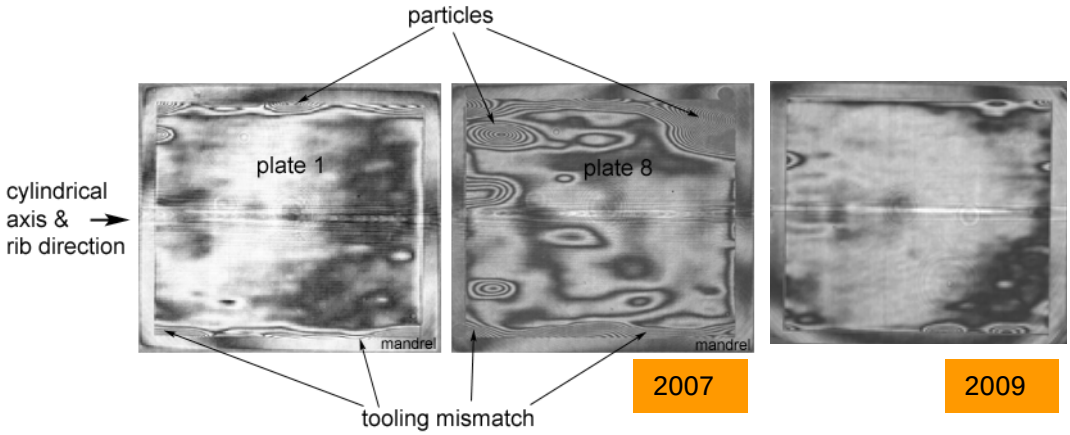

Figure 18: Example of interferogram as obtained at the beginning of this activity, measured on the first plate and on the eighth plate of HPO-0196, respectively. The wavelength of the HeNe laser used by the interferometer is 633 nm and the plate dimensions are 66 × 66 mm^2. The first plate of a stack could achieve in 2007 only a 90% bonded area to the base plate. With increasing stack height, the residual figure errors at the edges of the stack grow towards the centre of the stack. In addition particulate contamination starts to further decrease the shape match between the next plate to be stacked and the top plate of the existing stack, thereby decreasing the chance of achieving a good bond. The right most picture shows the latest 2009 data, demonstrating the significant improvement in plate cleanliness and bond quality. The horizontal feature in the centre of the plates is an artefact generated by the nulling lens.

Figure 19 shows a comparison of the stacking and cleaning process flow as used in the previous activity and as developed for this activity. In the previous activity the only way to determine the cleanliness of a plate was by evaluating the interferogram after that a plate had been bonded. This meant that an entire stack had to be abandoned at plate *n* if that plate showed a large trapped particle. To improve efficiency we developed a process where the plate is inspected before stacking, which required a particle detections system operating on plate level.

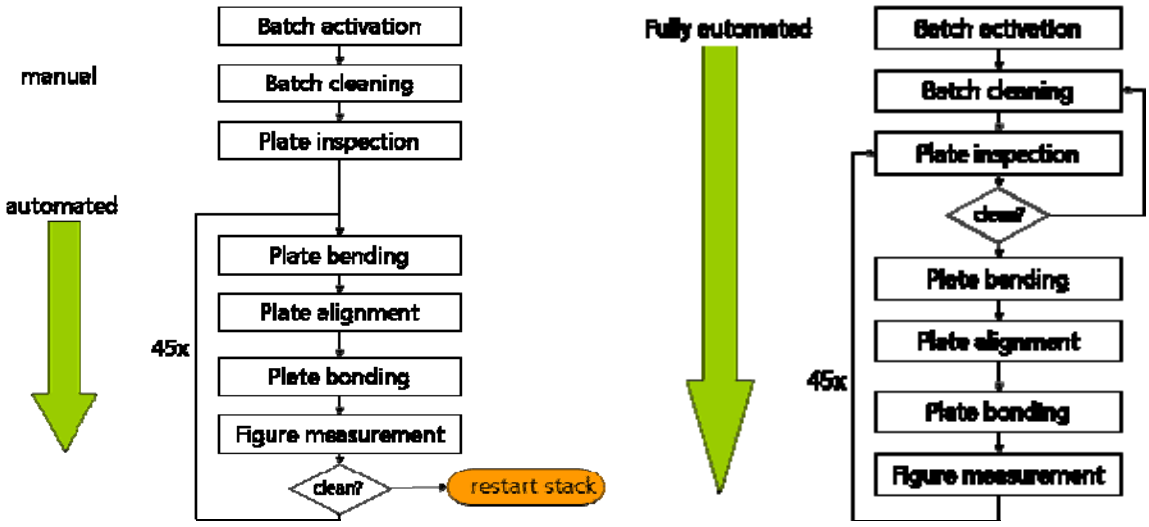

Figure 19 Left: Partial manual stacking process as used in the previous activity. Right: New cleaning and stacking process as developed for this project.

The requirements for such a particle detection system are to detect particles with a diameter of 0.1 micrometer or larger. In order not to delay the stacking process, such a system would need to be fast and in-line with the stacking robot.

We have developed such a particle detection system that can handle rectangular plates with sharp edges, which combines a special high brightness LED light source, an elliptic condenser and a line CCD. The principle of the system is to detect light scattered by particles, scratches or digs.

6.2 Stacking robot

The stacking robot is a fully automated system which is specifically developed to stack SPOs and which is a combination of standard semiconductor systems and newly developed tools. This robot has been completely redesigned and the latest, 3rd generation is operational since February 2009. The complete system has a footprint of a few m^2 only and is installed in a class 100 clean area. The process is summarised as follows:

A batch of plates is being cleaned and mounted inside a cleaning container, next to the stacking robot. Note that coating is done before plate cleaning and therefore integrated in the presented work flow. In the centre of the stacking robot a robotic arm is located which handles the plates between the different process steps, after the initial plate cleaning step (see Figure 20).

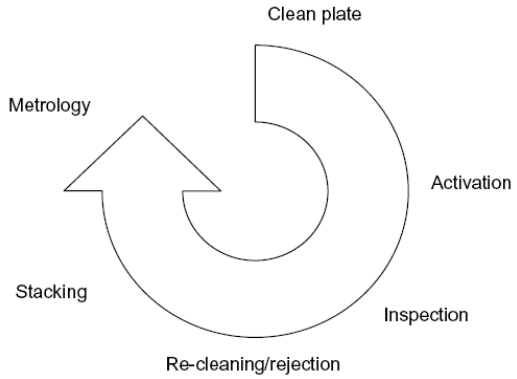

Figure 20 Cleaning and stacking operation principle

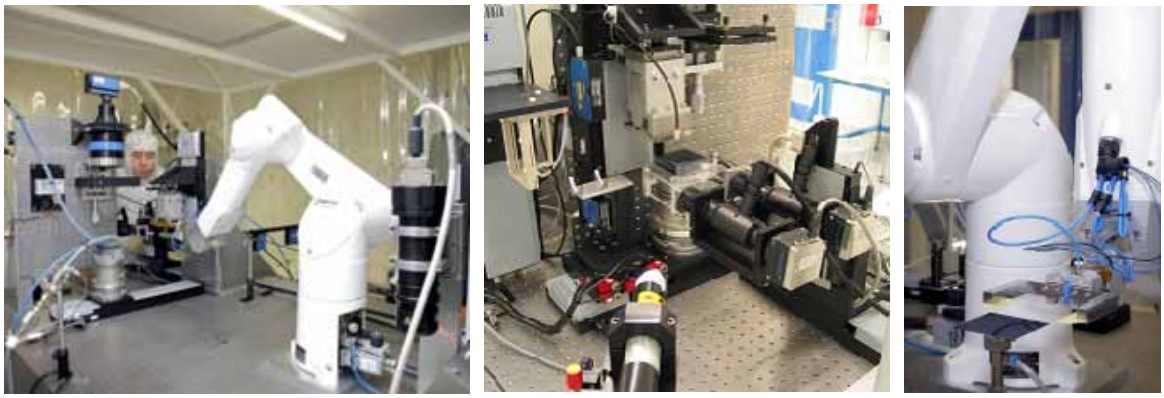

Figure 21 Stacking robot inside the class 100 clean area at cosine. The system is installed on a vibration isolated table, consists of more than 16 axes, is fully automated and is designed to build stacks up to 100 plates high. The plates can be positioned with μm accuracy and automatically be bent into the required shape.

The robot then selects a plate and inspects it for particles. The wafer industry has many tools to inspect wafers with round edges, however for rectangular plates with ribs and sharp edges no such tools exist. We have now developed a particle detection system (PDS) based on scattered light that can detect within a few minutes on both the ribbed and the reflective size of a plate particles down to a size of 0.8 μm. Further systems to detect down to 0.1 μm particles are under development. Using the PDS it was also shown that our processes do not contaminate the plates

during the stacking operation and that the limit to the cleanliness is rather determined by the initial cleaning step.

After inspection, the robot takes, based on the residual particle count, a decision whether to proceed with the plate or whether to reject it. The plate is then handed over to the actual stacking tool, which will elastically bend it into a cylindrical or conical shape. This tool, called a die, is then lowered onto the mandrel where it will deposit the plate or stack it onto already existing ones. The die and the mandrel are supervised by metrology systems based on auto-collimators, cameras and force sensors. We have also now integrated force measurement into the die in order to measure the dynamics of the stacking process in-situ while stacking. After the plate has been stacked, its figure is measured using an interferometer equipped with a computer generated hologram acting as nulling lens. Figure errors can be measured to $\lambda/20$ and the surface deviation measurements indicate whether residual particles have been caught and what size they had.

At the end of the stacking process development a number of stacks (see Figure 23) were assembled and integrated into mirror modules. For the first time we have also stacked fully wedged plates, demonstrating for the first time fully focusing silicon pore optics modules.

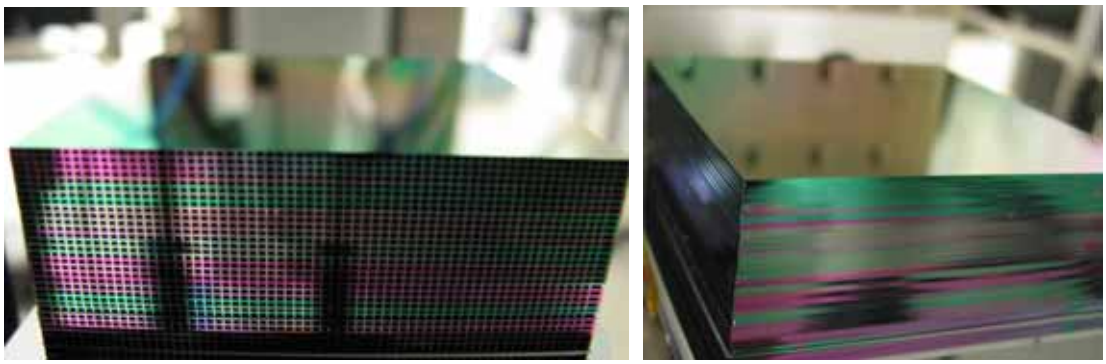

Figure 22 Example of one HPO, consisting of 30 wedged plates stacked on top of each other. The color differences are caused by interference of the light with the wedge layer.

6.3 Stacking process summary

1. The new stacking robot XOAT-3 is fully operational and has significantly improved on the quality of the stacking.
2. We have produced fully wedged stacks up to 30 plates high and have demonstrated the new double-sided wedging technique, required to meeting the IXO requirements. This also demonstrates that the transfer of the plate manufacture process from a former manufacturer to Micronit was successful.
3. The plate production process needs further development to reduce the number of trapped particles and to reduce the amount of damages to the edges, causing false positives in the particle detection system.
4. The X-ray performance of the first 10 plates of an HPO have significantly improved. The stacks achieve in single reflection a HEW of 7” on the first 9 plates, which corresponds for a mirror module in double reflection to 10”. This compares to 17” on the first 4 unwedged plates measured in 2007 and demonstrates the significant improvement in stacking quality. The complete first plate exhibits in single reflection a HEW of 4.2”.

7 Mirror module integration

7.1 Integration

The mirror module integration process remained unchanged and identical to the process developed in the previous activity: Two stacks (one representing the parabolic and one the hyperbolic part of a Wolter-I optic) are co-aligned using an X-ray pencil beam. This allows testing the optics at the wavelength they will later operate. The most critical alignment, the kink angle, can be set to sub arc second accuracy. Once aligned, two Cesic® brackets are glued to the sides of two stacks, hence forming a stiff mirror module which is essentially a lens. Because of being a lens it relaxes significantly the alignment requirements for integration into a petal.

The XOU integration is performed at the FEM beamline of the PTB laboratory at the BESSY synchrotron radiation facility. This beamline has a vacuum tank with a hexapod on which a XOU mounting structure is placed. The XOU mounting structure is equipped with a 6-axis table. The hexapod is used to move all parts of the XOU that are fixed with respect to the mounting jig (i.e. the brackets) and the 6-axis table is used to move the stack with respect to the brackets.

The HPO's are characterized before integration with pencil beam measurements to determine the contribution of the individual HPO's to the XOU PSF. The XOU has been characterized before and after gluing to determine the contribution of gluing to the XOU PSF.

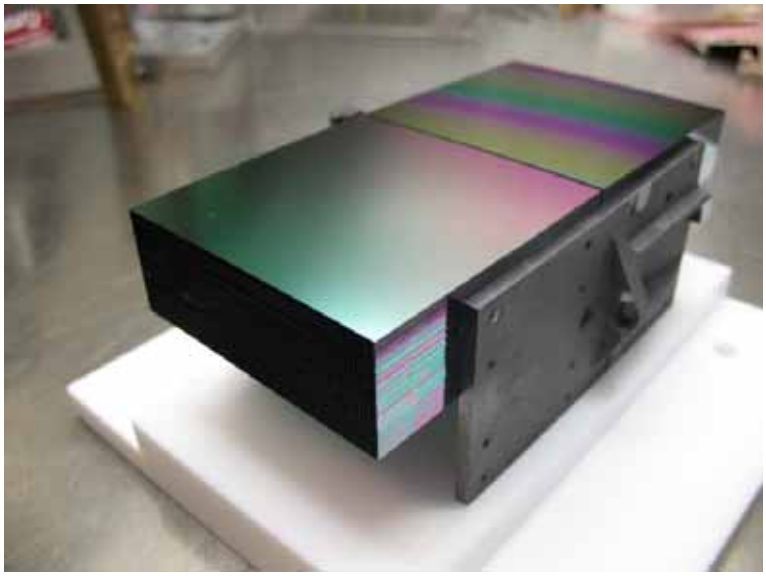

Figure 23 A mirror module in flight representative configuration, consisting of two co-aligned wedged silicon pore optics stacks, with two Cesic® brackets attached. The three fully isostatic mounting feet are not shown.

7.2 Mirror module mechanical design

The design of the mirror modules has been reviewed in order to check compatibility with IXO launch configurations. The Finite Element Model of the mirror module has been developed into more detail. The mechanical I/F has been improved to a fully isostatic mounting concept to cope with e.g. dynamic and thermo-elastic behaviour of the spacecraft structure (petal). The bracket material has been changed from MF CeSiC® to HB CeSiC® in order to meet the preliminary launch loads of up to 100 g. The first resonance frequency of the mirror module is clearly above the requirement of 200 Hz, regardless of the configuration of the mirror module, such as plate sizes and number of plates.

7.3 Cesic Elemental Cell

To measure the XOUs a representative mounting structure and test bed was built, which is capable to accommodate one XOU Mirror Module during X-ray performance and environmental testing. For transportation purposes a dedicated container is provided for the mounting structure with the assembled XOU.

The mounting structure is called CEC (CeSic® Elemental Cell). It is compatible with the design of the XEUS/IXO telescope petals of a previous study. The CEC provides on one side the interface to the XOU and on the other side of the I/F to the test H/W at the X-ray test facilities PANTER and BESSY.

The design of the CEC takes into account the requirements for thermal testing and for vibration testing of the mounted mirror module. However, neither the detailed environment, nor the final vibration test requirements are finally frozen so far. This is partly due to the change from XEUS to IXO. Therefore, reasonable assumptions have been made for loads and thermal environment, based on experience for similar space borne structures and based on engineering judgement.

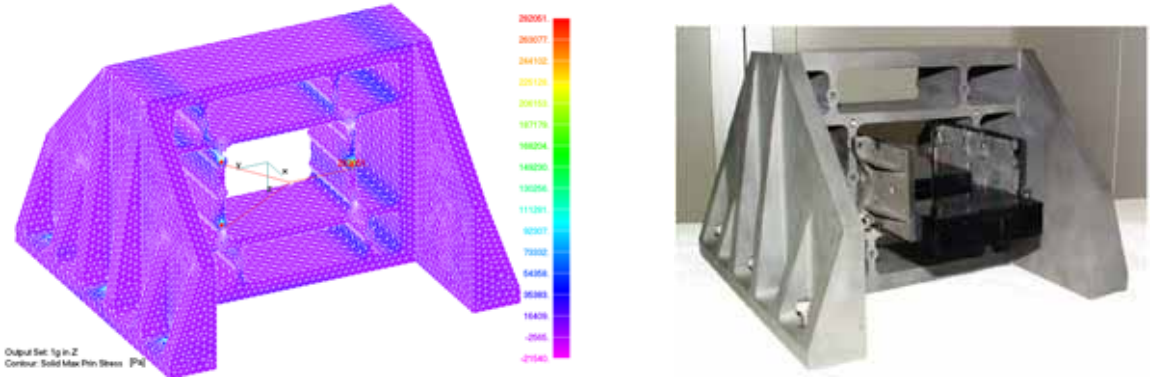

Figure 24 FE model (left) and as-built CEC (right), shown with a mirror module integrated prior to X-ray testing.

The CEC is a monolithic structure, made from HB-type CeSiC® from ECM. HB-type CeSiC® has a higher strength than MF=type Cesic®, which was initially selected for this application. During the course of the detailed design it was decided to switch from MF to HB material, to accomodate increased mechanical design loads at mirror module level of up to 100 g.

7.4 X-ray testing

The goal of these tests is to determine the optical quality of an XOU by measuring it under illumination by X-rays, with an X-ray detector at intra focal distances (note that no facility is available that could measure 50 m focal length X-ray optics). Pencil beam tests are performed at the PTB laboratory of BESSY and full area illumination at the PANTER facility of MPE.

The pencil beam measurements are used during alignment and integration of an XOU and are then used to predict its optical performance by reflecting a small X-ray beam at grazing incidence of the surface of every plate / pore. These measurements allow us to determine the angular deviation of the mirror surface in each pore of the XOU. Using raytracing algorithms, this allows us then to predict the PSF and HEW of the optic in the focal plane. In combination with the data taken from the individual HPOs this gives additional information on how stack up errors propagate, and help us in improving the stacking process.

The BESSY XOU test plan is split into three sub tests:

1. Measuring in double reflection the figure using an X-ray pencil beam

2. Imaging of the XOU using large field X-ray illumination (at BESSY)
3. Imaging of the XOU using large field X-ray illumination (at PANTER)

The figure of the individual HPOs is measured during stacking using interferometry. It is therefore considered part of the manufacturing.

PANTER is used to confirm, using full beam illumination, the pencil measurements taken at BESSY. Furthermore it allows to measure scattering off the ribs and to perform reflectivity as function of energy measurements.

7.5 Full area illumination (PANTER)

Measurements were performed with the PSPC as well as with the TRoPIC CCD camera.

The PSPC (Position Sensitive Proportional Counter) is a conventional multi-wire proportional counter filled with high-Z counter gas (65% Ar, 20% Xe, 15% CH_4) at a pressure of 1465 mbar. It has a circular sensitive area of 8 cm in diameter and can be operated in two different gain states depending on the applied high voltage. The position resolution is about 250 micron (160-600 μm depending on energy).

The PSPC can be moved by about +116.5 mm and -54.9 mm vertically to the optical axis of the facility. TRoPIC is an eROSITA prototype camera operating in frame-store mode and was specially developed for calibration measurements for eROSITA and high-energy missions like SIMBOL-X.

With a pixel size of 75 micron * 75 micron, a cycle time of about 50 ms, an out-of-time event fraction of only 0.2%, and a 256 * 256 pixel FOV (19.2 mm * 19.2 mm) it is well suited for PSF measurements and high-resolution imaging. Moreover, various gain levels are available to optimise the amplification according to the incident X-ray spectrum.

Figure 25 A mirror module mounted inside the PANTER tank in flight representative configuration in the CEC.

With a nominal focal length' of f=50 m and a distance r = 2 m from the optical telescope axis a XOU would create an image at a reflected distance of about k = 32 cm from the incident axis at an imaging length of v = 8 m; This distance k exceeds the vertical range of the PANTER focal plane instrumentation. The XOU was therefore mounted about a = 24 cm below the PANTER optical axis. At the nominal XOU incidence angle of about 34.36 arcmin (0.573 deg) double

reflections from the XOU would occur at the central range of the detectors, slightly shifted to the bottom, because the beam incident onto the XOU has an angle of about 8.9 arcmin below the PANTER axis. The rotate-tilt-stage with the XOU can be horizontally moved in and out of the beam.

One aperture stop allows illuminating individual plates, another one to simultaneously observe direct and reflected beam to determine reflection efficiencies.

Figure 26 shows a comparison of a mirror module assembled in the previous activity 2007 and one mirror module assembled in this activity. The figure shows a comparison of plates 1, 4, 8. The significant improvement in quality is clearly visible from the direct comparison of the double reflected image measured at 1.49 keV at a distance of 8 m.

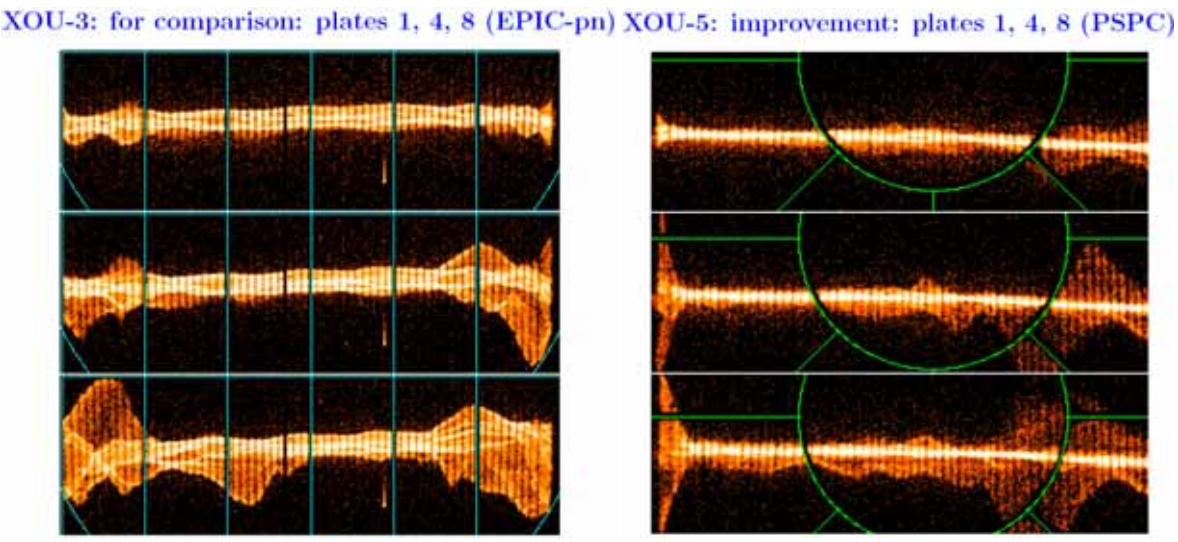

Figure 26 shows a comparison of PANTER measurements of XOU-3 (left) to XOU-5 (right). From top to bottom plate 1, 4 and 8 are shown, measured at an energy of 1.49 keV. The significant improvement in quality is clearly visible from the direct comparison of the double reflected image measured at 8 m.

The mirror module (Figure 26) has 22 measured reflecting plate pairs and one can calculated the measured effective area

$$A_{eff,meas} = \varepsilon \cdot \mathrm{A}_p \tag{4}$$

where the illuminated area is

$$A_p = n \cdot w_p \cdot h_p \tag{5}$$

with n the number of illuminated plate pairs, w_p the width of the plates (65.8 mm) and h_p the height of the plate (0.775 mm).

The measured effective area can be compared to the expected effective area

$$A_{eff,\exp} = A_{geom} \cdot n \cdot \frac{l_{opt}(f,r)}{l_{plate}} \cdot \tau \cdot R^2(E) \tag{6}$$

with l_{opt} being the optimum length of the plates at a radius r and for a focal length f, l_{plate} being the actual length, R the reflectivity at energy E, A_{geom} being the open area of one plate (i.e. area of all pores added up) and τ a factor for other known geometric blocking contributions (known stacking or stack misalignment errors).

All geometric influences can be calculated easily, difficult to derive is the reflectivity value at a certain energy, as it depends on the roughness, the incidence angle and the surface composition. The roughness of plate level oxidised wedged plates has been measured using reflectometry at BESSY to be 0.5 - 0.6 nm. The surface composition of a wedged plates is not trivial to define. We assume SiO_x with x being very close to 2. In the absence of measured reflectivity data (note that all reflectometry so far has been performed at 6 to 10 keV and that it is recommended to perform in the future reflectometry also at the same energies that PANTER is using, i.e. 2980 eV) the reflectivity is modelled using SiO_2 with a 3% reduction in density, so 2.15 g/cm^3.

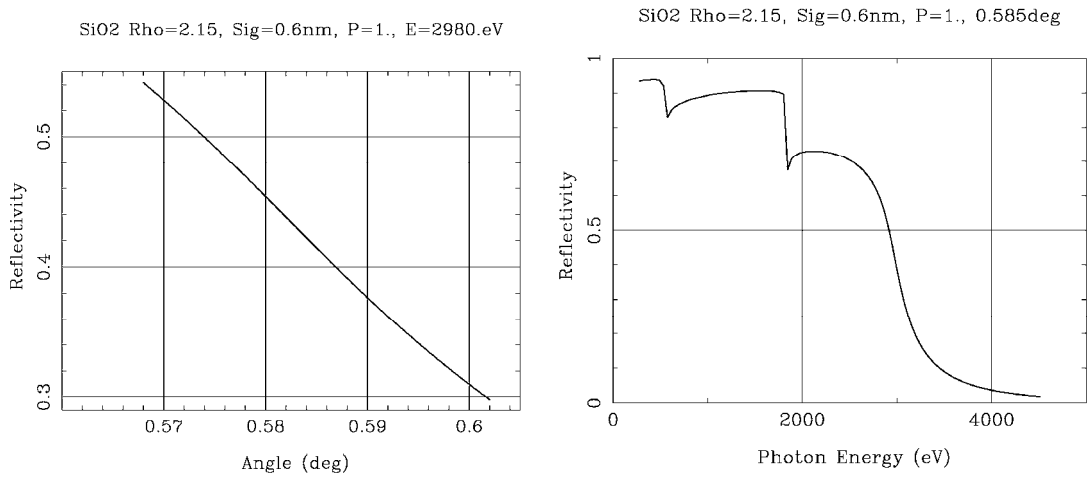

Figure 27: Left: Reflectivity of SiO_2 (with a reduced density of 2.15 g/cm3 to model the wedged surface) as a function of grazing incidence angle at 2.98 keV. Right: Reflectivity as a function of energy at an angle of 0.585 deg. Data from http://henke.lbl.gov/optical_constants.

The biggest uncertainty in these measurements comes from the incidence angle. During alignment at PANTER the throughput at 0.28 keV was maximised, resulting in an approximate incidence angle (the beam divergence due to the finite source distance has little influence on the limited number of plates) of 34.4 arcmin (0.573 deg), with an accuracy of 1-2 arcmin. While this has no significant influence at lower energies, at 2.98 keV an error of 1 arcmin already changes the reflectivity by ~5% (see Figure 27).

The measured efficiency for different energies and the resulting measured effective area, using eq. 5, of XOU-5 is shown in Table 1. To calculate the expected effective area we use eq. 6, with

A_{geom} = (62 × 0.83 mm + 2 × 1.37 mm) × 0.605 mm = 32.791 mm^2

n = 20

l_{opt} = 58.00 mm

l_{plate} = 65.77 mm

τ = 1 (perfect stack to stack alignment)

and the reflectivity R taken from Figure 27. This results in an expected effective area as shown in Table 1. We see that the measured effective area is only a few percent lower than the expected one, without even considering small misalignment errors (τ) between the two mirror modules, which are typically a 1-2 percent. These values give confidence that the wedged plates reflect as good as the unwedged ones. However, future, more detailed measurements using coated plates will yield further insights.

Table 1: Measured effective area of XOU-5 (plate level oxidised wedged plates Micronit).

Energy	**eV**	**280**	**1490**	**2980**
Measured effective area	mm^2	529	484	107
Measurement error	%	0.2	0.2	0.04
Reflectivity SiO_2 @ 0.6 nm (rms)		0.935	0.906	0.42
Expected effective area	mm^2	557	523	112
Measured / expected		95%	93%	95%

7.6 Pencil beam testing (BESSY)

The FEM beamline consists of a fixed monochromator centred at an energy of 2.8 keV, and a combination of slits and pinholes to collimate the X-ray beam. A PI M-840.5DG hexapod is installed inside a vacuum chamber (base pressure 10^{-6} mbar), which allows translating (1 μm step size, 2 μm repeatability) and rotating samples in all 6 degrees of freedom. Rotation of the hexapod is monitored by an external Moeller-Wedel autocollimator and any deviations are corrected during the measurements using a closed loop. The X-ray beam can be detected either by using a Si-diode at a distance of 400 mm from the sample or by using a Peltier-cooled Princeton Instruments XCCD (1340 x 1300 pixels, 24.1 μm pixel size) in combination with a 10 μm thick phosphor screen at a distance of 5.0 m from the hexapod. The XCCD is outside the vacuum chamber and can be computer-controlled translated in vertical direction by 300 mm and in horizontal direction by 50 mm. The beam line has several slits and pinholes, which allow performing pencil beam measurements down to 50 μm size and full illumination measurements up 7×7 mm.

The standard measurement is to test stacks and mirror modules

- at an energy of 2.8 keV
- with a pencil beam of 0.1 × 0.1 mm^2 (HEW 4")
- in vertical steps of 0.052 mm (0.78 mm / 15)
- in horizontal steps of integer numbers of pores (integer number of millimetres)
- under an incidence angle of 0.573 deg (for a radius of 2000 mm)

Using this measurement procedure we have measured wedged stacks produced by the new stacking robot (see Figure 28): The first plate, measured at an energy of 2.8 keV, has a point spread function (PSF) with a HEW of 4.2". The first 9 plates have a PSF with a HEW of 7", which correspond in double reflection to a HEW of 10". The full length of the plates was scanned and the scans where repeated every 2 mm over the full width of the plate.

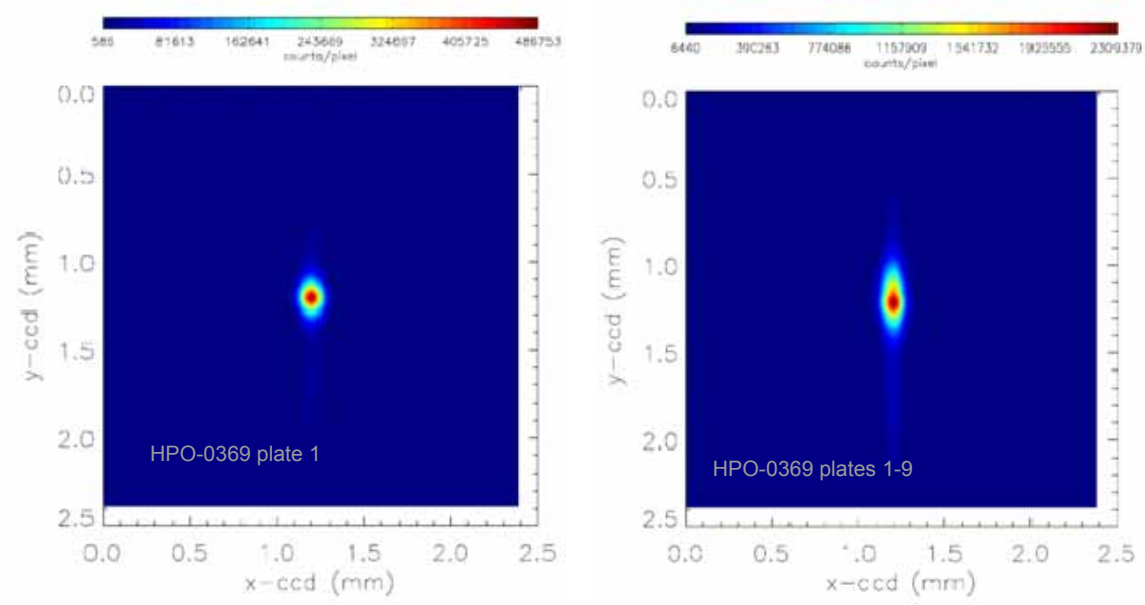

Figure 28 LEFT: PSF of the first plate of a stack of 9 wedged plates measured using established procedures in single reflection at 2.8 keV at the FEM beamline in the PTB lab at the BESSY synchrotron radiation facility. The full length of the plate was scanned using a 100 μm pencil beam with an intrinsic HEW of 4". The scans where repeated every 2 mm over the full width of the plate. The resulting PSF excluding the direct beam has a HEW of 4.2". RIGHT: The same measurement repeated on the entire stack of 9 plates. The HEW of the PSF excluding the direct beam is 7". In double reflection this would result in a HEW of a mirror module of 10".

In November 2009 a mirror module was then measured in double reflection, mounted inside the CEC in flight representative configuration (see Figure 24). From the results measured at 5 m one can extrapolate an estimate for the PSF expected at 50 m, shown in Figure 29 for the first 4 and for 20 plates.

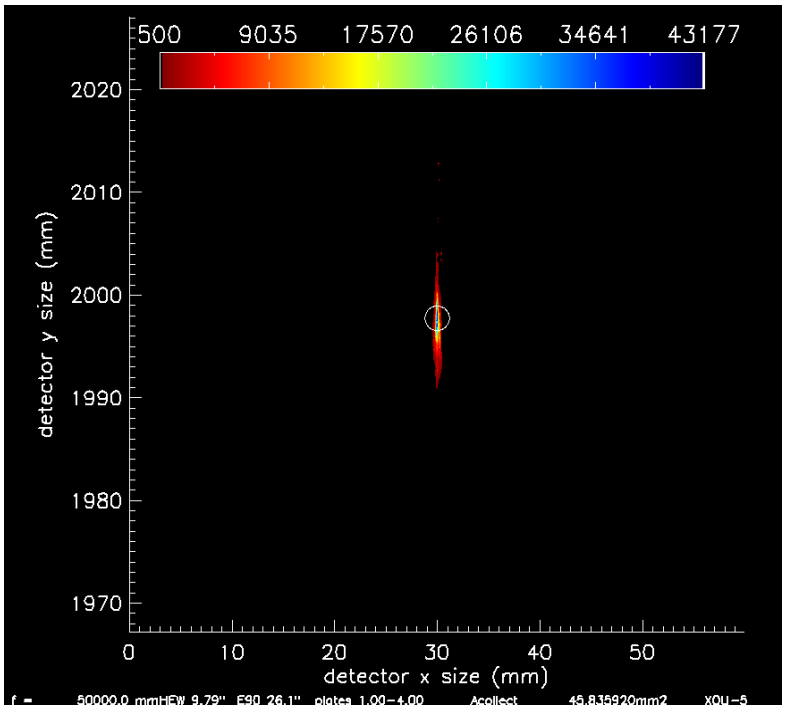

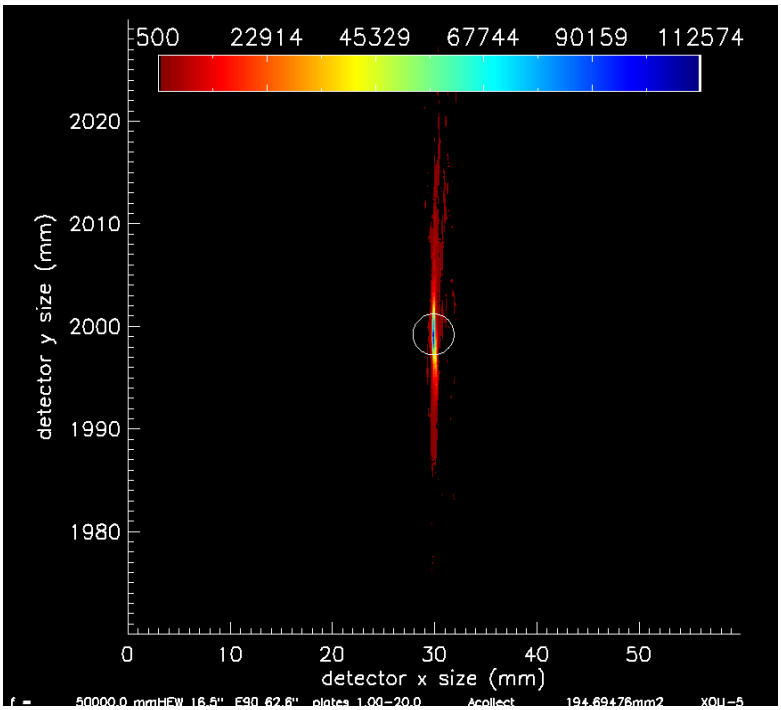

Figure 29: PSF of the first 4 (top) and 20 (bottom) plates of a mirror module consisting of 20 wedged plates measured using established procedures in double reflection at 2.8 keV at the FEM beamline in the PTB lab at the BESSY synchrotron radiation facility. The full length of the plate was scanned using a 100 μm pencil beam with an intrinsic HEW of 4". The scans where repeated every 2 mm over the full width of the plate. The resulting PSF excluding the direct beam has a HEW of 9" (4 plates) and 16" (20 plates).

Figure 29 it can been seen that the mirror modules produced in this activity are measured using 3 keV X-rays in mounted configuration in double reflection, extrapolated to 50 m, a performance of

- 4 plates @ 10" HEW (9" without direct beam)
- 20 plates @ 16" HEW (16" without direct beam)

Not shown, but also analysed where the first 10 and 15 plates, which yield

- 10 plates @ 12" HEW (11" without direct beam)
- 15 plates @ 13" HEW (12" without direct beam)

7.7 X-ray metrology conclusions

A mirror module of the latest generation has been measured in double reflection both at BESSY and at PANTER, mounted in flight representative configuration. XOU-5 is the best XOU built so far, fully consisting of wedged plates.

- The effective area measured on the uncoated modules is over the measured energies almost constant and is only 6-7% lower than expected, not even considering small misalignment errors between the two stacks. These few percent loss is a value similar to the results obtained also on previously flown X-ray optics.
- The mounted optics have an angular resolution of
  - 4 plates @ 10" HEW (9" without direct beam)
  - 10 plates @ 12" HEW (11" without direct beam)
  - 15 plates @ 13" HEW (12" without direct beam
  - 20 plates @ 16" HEW (16" without direct beam)

For comparison one should note that from the previous activity the best results where achieved 2007 with XOU-3. It had the first 4 plates @ 17" with a wedge added artificially in the data analysis, since at that time no wedged plates where yet available. Therefore both the MPE and PTB test facilities confirm the significant increase in the quality of the mirror modules compared to the ones built in the previous activity.

8 Future work

The stacking robot was initially designed to demonstrate the technology for XEUS, which had a focal length of 50 m, at a radius of 2 m. With the transition to IXO the focal length has been reduced to 20 m with a maximum outer radius of 1.9 m. This means that the required plate length for IXO, at a pore height of 0.605 mm, ranges from about 170 mm for an inner radius of 0.4 m to 26 mm at an outer radius of 1.9 m.

In the next year a second stacking robot will be built to stack plates with the same length but at a radius of 0.74 m. Additional automated plate inspection systems are being developed and installed to further improve on the cleanliness of the silicon plates, which will allow the stacks to perform significantly better than 4". Simultaneously PTB will upgrade the X-ray test beamline at BESSY II for ESA to allow measurements at a distance of 20 m, in the focal plane of the IXO optics. Similarly, the PANTER facility will also be extended for longer focal lengths. Environmental testing will be prepared by performing additional pull tests on plate and stack level. These preparations also include bracket light weighting and optimisation for integration and operation of stacks at room temperature. Note that so far the production chain was demonstrated for the more demanding XEUS requirement of integration at room temperature and operation at 150 K, whereas IXO will operate at or close to room temperature.

In the mid term future industrialisation of the entire production process will be pushed forward. The stacking systems are already now fully automated, but require improvement in the stacking time and redundancy of the system. The yield has to be further increased and we will perform first tests with stacks with a curvature in longitudinal direction, which will allow overcoming the limits imposed by the conical approximation.

9 Conclusions

An ESA TRP activity was carried out by cosine Research (NL), Micronit (NL), Kayser-Threde (DE), SRON (NL), DTU (DK) and MPE (DE) with the goal of improving the angular resolution of Silicon Pore X-ray Optics. Silicon Pore Optics is the European baseline mirror technology for the International X-ray Observatory (IXO), one of the three L-class mission candidates under the Cosmic Vision 2015-2025 program.

The entire production chain of these light-weight and modular X-ray optics has been reviewed, improved, demonstrated and tested, from silicon plate manufacture, over ribbing, dicing, wedging, coating, stacking, assembly and integration up to petal level.

A simplified process flow to manufacture stackable Si mirror plates is demonstrated, with an emphasis on reduced manufacturing cost. An important factor is the consideration of standard wafer processes and equipment. This activity has shown ways to enable manufacturing the required 200 000 silicon plates for IXO in a cost-effective manner within the allocated time-scale.

Customized wedging equipment is used to taper plates to the correct geometry, and industry-standard oxidation and wet chemical processes are used to ensure bondable surfaces. An analysis of the relevant tolerances has led to the optimization of the wedging process in order to meet the requirements of the IXO.

Two methods to apply structured coatings have been developed and stacks with Ir and C overcoating were demonstrated. Reflectometry measurements were performed to demonstrate that the silicon plates, after all processing steps and including coating have a rms surface roughness of 0.5 nm.

A new generation of the automated stacking robot has been developed. Using this robot, stacks with a radius of curvature of 2 m consisting of fully wedged plates have been built and were measured at the BESSY synchrotron radiation facility.

The complete first plate exhibits in single reflection a HEW of 4.2". In double reflection a HEW of 9" on the first 4 plates and 16" on the first 20 plates was measured on mirror modules mounted in flight representative configuration. This compares to 17" on the first 4 unwedged plates measured in 2007 and demonstrates the significant improvement in stacking quality.

The activity was centred on improving the technology at a radius of 2 m for a focal length of 50 m, conform the initial requirements. At the end of the project, a detailed study on the requirements to produce modules at inner radii and shorter focal length has been carried out. First considerations about inner radii modules as required for IXO and re-calculation of effects of launch loads on mirror modules were all concluded successfully.

So far no show stopper has been identified that would impede improving the performance of silicon pore optics beyond 5".